# Radiation activates the NORAD expression to promote ESCC radioimmunotherapy resistance via EEPD1/ATR/Chk1 signaling by inhibiting the pri-miR-199 processing and exosomal transfer of miR-199a-5p

**Yuchen Sun**
Xi'an Jiaotong University Medical College First Affiliated Hospital
**Jizhao Wang**
Xi'an Jiaotong University Medical College First Affiliated Hospital
**Xuanzi Sun**
Xi'an Jiaotong University Medical College First Affiliated Hospital
**Jing Li**
Xi'an Jiaotong University Medical College First Affiliated Hospital
**Xu Zhao**
Xi'an Jiaotong University Medical College First Affiliated Hospital
**Yuan Ma**
Xi'an Jiaotong University Medical College First Affiliated Hospital
**Xiaobo Shi**
Xi'an Jiaotong University Medical College First Affiliated Hospital
**Fengyi Qu**
Xi'an Jiaotong University Medical College First Affiliated Hospital
**Xiaozhi Zhang** ( zhangxiaozhi@mail.xjtu.edu.cn )
Xi'an JiaoTong University

**Research Article**

**Keywords:** Esophageal squamous cell carcinoma, Radioresistance, NORAD, pri-miR-199a, EEPD1

**Posted Date:** May 14th, 2021

**DOI:** https://doi.org/10.21203/rs.3.rs-516399/v1

# Abstract

**Background** Radioresistance, a poorly understood phenomenon, results in the failure of radiotherapy and consequent local recurrence, threatening a large proportion of ESCC patients. To date, lncRNAs have been found to be involved in diverse biological processes, including radioresistance.

**Methods** ELISA was used to evaluated the H3 modifications in radio-resistant ESCC cells. FISH and qRT-PCR were adopted to examine the expression and localization of lncRNA-NORAD, pri-miR-199a and miR-199a. Electron microscopy and Nanoparticle tracking analysis (NTA) was conducted to observe and identify exosomes. High-throughput RNA sequencing and TMT mass spectrometry were performed to identify the functional lncRNAs and proteins involved in ESCC radioresistance. A series of in vitro and in vivo experiments were performed to investigate the biological effect of NORAD. CHIP, qPCR-RIP, co-IP and dual-luciferase reporter assays were used to explore the interaction of related RNAs and proteins.

**Results** We show here that a DNA damage activated non-coding RNA-NORAD, which is critical for ESCC radio-resistance. NORAD was highly expressed in radio-resistant ESCC cells and tissues. Irradiation treatment promotes NORAD expression via enhancing H3K4me2 enrichment on its region. NORAD knockdown cells exhibit significantly hypersensitivity to irradiation *in vivo and in vitro*. NORAD is required for initiating repair and restart of stalled forks, G2 cycle arrest and homologous recombination repair upon irradiation treatment. Mechanistically, NORAD inhibits miR-199a expression by competitively binding PUM1 from pri-miR-199a, inhibiting the process of pri-miR-199a. Mature miR-199a in NORAD-knockdown cells can be packaged into exosomes; miR-199a restores the radiosensitivity of radioresistant cells by targeting EEPD1, then inhibiting ATR/Chk1 signaling pathway. Simultaneously, NORAD knockdown blocks the ubiquitination of PD-L1, leads to the better response for radiation and anti-PD-1 treatment in mouse model.

**Conclusion** This study raises the possibility that LncRNA-NORAD could be a potential treatment target for improving the efficiency of immunotherapy in combination with radiation in ESCC.


# Background

Esophageal cancer, one of the most lethal malignancies worldwide[1], is mainly histologically classified into esophageal adenocarcinoma (EAC) and esophageal squamous cell carcinoma (ESCC). In Asian countries, ESCC is the most common histological type and has a worse prognosis than EAC. Although surgery is the most effective treatment for prolonging survival, a large number of patients are not candidates for direct esophagectomy[2-4]. Comprehensive therapy, including radiation and chemotherapy, is introduced to either improve the effects of surgery or control the growth of cancer lesions in nonresctable patients. Radiation is an important part of combined therapy, serving as an efficient way to control local recurrence and optimize surgery strategies. For example, preoperative chemotherapy combined with radiotherapy is required for cervical esophageal cancer to avoid simultaneous laryngectomy[5]. Both definitive and preoperative radiation are important therapeutic strategies in

prolonging the overall survival of patients with ESCC[6]. A high local recurrence rate accounts for the relatively poor prognosis of ESCC patients. Although chemoradiotherapy tremendously reduces the local recurrence rate, approximately 40%-60% of patients still experience local recurrence after concurrent chemoradiotherapy[4, 7], partially due to radiation or chemotherapy resistance. Although terrific progress has been made in identifying novel biomarkers and therapeutic targets for improving radiation sensitivity, the molecular mechanism underlying radioresistance remains ambiguous and complex; it is thought to involve cell cycle checkpoints that prevent cancer cells from sustaining radiation-induced DNA damage, activation of the DNA damage response, the self-renewal of cancer stem cells, epithelial-mesenchymal transition(EMT), etc.[7, 8]. In this manuscript, we aimed to identify key genes that participate in sensitizing ESCC cells to radiation therapy and to lay the foundation for drug development.

In recent years, long noncoding RNAs (lncRNAs) have attracted great attention as a result of their diverse biological functions in the development and progression of multiple cancers[9]. To explore key lncRNAs that are involved in ESCC radioresistance, we performed RNA-sequencing analyses to identify differentially expressed lncRNAs between radioresistant ESCC cells and control cells. Combined with our previous studies, the DNA damage-activated noncoding RNA-NORAD (also named linc00657) garnered our attention. NORAD is abundantly expressed in multiple eukaryotic cells, is conserved across mammalian species and has been shown to play oncogenic roles in numerous cancers. NORAD maintains genomic stability by sequestering and negatively regulating PUMILIO proteins through its 18 conserved PUMILIO response elements [10]. Another study reported that NORAD interacted with DNA damage-repair- and DNA replication-related proteins, assembling a topoisomerase complex to sustain genomic stability in response to DNA damage[11]. In addition, NORAD binds to a group of microRNAs, modulating their abundance to exert oncogenic functions[12] [13]. In our previous study, we identified that NORAD knockdown significantly sensitized ESCC cells to radiation. However, how NORAD regulates radiobiological processes in ESCC is unclear.

The main anticancer mechanism of radiation is the generation of a cluster of lethal lesions, which in turn induce DNA damage in cells and tissues [14] Damaged DNA can be repaired by the activation of homologous recombination (HR) and nonhomologous end joining (NHEJ) pathways in vitro [15]. The crosstalk between DNA damage repair and radiosensitivity is obvious [16]; our previous studies showed that NORAD expression can be induced by radiation treatment in ESCC cells. Furthermore, some studies have found that inhibiting DNA damage repair enhances the efficiency of immune checkpoint therapy, especially when combined with radiotherapy. Frank P et al reported that the ATR kinase inhibitor AZD6738 reduced the exhaustion of CD8+ T cells induced by radiation. In addition, AZD6738 combined with radiation can generate immunologic memory for tumors in mice [17]. The latest study found that DNA double-strand breaks promoted PD-L1 expression by activating STAT1 and STAT3 signaling [18]. TMT-based proteomics analyses also suggest the potential function of NORAD in regulating the immune response. However, how suppressing DNA damage repair responses can amplify immune checkpoint therapy efficiency in combination with radiotherapy remains elusive. In this context, we hypothesize that NORAD modulates ESCC radiosensitivity by regulating the DNA damage repair process. We assumed that NORAD is involved in the synergy between radiotherapy and immune checkpoint therapy.

# Methods

### 1. Cell culture, Lentivirus infection and transfection

The esophageal squamous carcinoma cell lines KYSE-150 and TE-1 were purchased from the Cell Bank of the Chinese Academy of Sciences Typical Culture Preservation Committee (Shanghai, China). Cells were maintained in Roswell Park Memorial Institute (RPMI) 1640 medium supplemented with 10% FBS and 1% penicillin/streptomycin. Cells were cultured in a 5% CO2 incubator at 37°C. Radioresistant cells were generated from parental KYSE-150 and TE-1 cells by seeding the cells into 6-well plates and then exposing them to radiation at a dosage of 2 Gy per day for 30 days. The surviving cells were characterized as radioresistant cells (termed KYSE-150R and TE-1R cells). The generation of radioresistant cells was validated by colony formation assays.

sh-NORAD lentivirus, sh-EEPD1 and their corresponding control lentivirus were purchased from Genechem (Shanghai, China). miR-199a-5p mimics, miR-199a-5p inhibitors, siRNA against PUM1 and EEPD1-expressing vector were purchased from GenePharma (Shanghai, China). For virus infection, KYSE-150 and TE-1 cells were seeded into 48-well plates and grown to 50% confluence. Lentivirus ($1\times10^8$ TU/ml) and infection reagents were mixed and added to the cells. The medium was changed after 48 hours of infection, and puromycin (3 μg/ml) was added to the medium to select cells that were successfully infected. Transient knockdown or overexpression of candidate genes was achieved by transfection of relative siRNAs or gene overexpression plasmid. Transient transfections were performed by using Lipofectamine 3000(Invitrogen/Thermo Fisher Scientific) according to standard protocol.

### 2. qRT-PCR

Total RNA was extracted from KYSE-150 and TE-1 cells using TRIzol reagent (Invitrogen, Carlsbad, CA, USA) and then reverse transcribed into cDNA using a PrimeScript™ RT reagent kit (TaKaRa, Dalian, China). MicroRNA-specific cDNAs were generated by using an EvoM-MLV RT kit. qRT-PCR was carried out using SYBR Premix Ex TaqTM II (TaKaTa, Dalian, China). GAPDH and U6 were used as reference genes for mRNA and microRNA, respectively.

### 3. Western blot

Total protein from KYSE-150 and TE-1 cells was extracted by RIPA buffer (Sigma Aldrich, Cambridge, MA) and quantified by BCA (Sigma Aldrich, Cambridge, MA). Then, proteins were subjected to SDS-PAGE through 10% gels and transferred onto PVDF membranes, which were then incubated with primary antibodies at 4℃ overnight. Secondary antibodies were then incubated with the membranes for 1 hour at room temperature before the protein bands were visualized using an ECL kit.

### 4. Extraction and identification of exosomes

Electron microscopy was used to observe and identify the extracellular vesicle-like structure of exosomes. Nanoparticle tracking analysis (NTA) was conducted to test the particle size-concentration distribution on

a ZetaView PMX 110 (Particel Metrix, Germany). CD63 was considered an exosome marker, and protein expression was evaluated by western blot. For the exosome tracer experiment, 2000 cells/well were seeded in a 96-well plate; the exosome suspension was incubated with 2 μM PKH26 for 5 minutes at room temperature and added to the target cells in a volume of 20 μl/well. The red fluorescence indicates the process of exosomes entering target cells.

### 5. Fluorescence in situ hybridization

We used KYSE-150 and TE-1 to produce cell slides, which were pretreated with HCl and then fixed with neutral formalin. A probe targeting NORAD was used for hybridization with cell slides after treatment with diluted prehybridization solution. DAPI was used to stain nuclei, and cell slides were observed by confocal microscopy.

### 6. Immunofluorescence

KYSE-150 and TE-1 cells were seeded on glass sides in 48-well plates and cultured overnight. Cells on the slides were fixed with 4% paraformaldehyde before they were treated with Triton X-100 (5%) to permeate cells and BSA solution to block nonspecific binding. Cells were treated with primary antibodies and incubated at 4°C overnight. After unbound primary antibody was removed, the cells were then incubated with PE-conjugated secondary antibody for 1 hour at 37 ℃. DAPI was added to the slides for nuclear staining, and glycerin was used to block the slides. Images of the slides under a confocal microscope were obtained. The primary antibodies and PE-conjugated secondary antibody were purchased from Abcam.

### 7. co-IP

Cells were lysed at 4°C for 5 min in RIPA buffer, containing protease inhibitors. Whole cell lysates were then precleared with protein A/G beads. PD-L1 antibody was then added overnight at 4 ℃ . The antibody/antigen complex was pulled out of the lysates by using protein A/G-coupled agarose beads. Beads were washed by RIPA buffer for 3 times and resuspended by 2loading buffer. The Western blot and assays were described in previous.

### 8. RNA immunoprecipitation (RIP)

We purchased a Magna RIP™ RNA-binding Protein Immunoprecipitation Kit (Millipore, Billerica, MA, USA) to analyze the interaction between RNA and proteins. KYSE-150 cells were lysed in RIP lysis buffer for further experiments. We used Ago2 antibody for immunoprecipitation and IgG antibody as the negative control. The expression levels of NORAD and pri-miR-199a were evaluated by qRT-PCR.

### 9. Homologous recombination (HR) reporter assay

HR reporter and I-SceI expression plasmids were purchased from Genechem (Shanghai, China). For the HR reporter assay, KYSE-150-sh-NC and KYSE-150-sh-NORAD cells were transfected with the HR reporter.

G418 (1 mg/ml) was used to select successfully transfected cells. Then, these cells were transfected with the I-SceI plasmid to induce double-strand breaks on the HR reporter plasmid. Cells were harvested for analysis after 48 hours. Cells that underwent HR repair are positive for green fluorescence positive. Lentiviruses containing sh-NORAD and sh-NC used here were not fluorescently labeled.

### 10. Apoptosis and cell cycle analyses

We used an Annexin V-APC 7-AAD Apoptosis Detection Kit I (BD Pharmingen TM, New Jersey, USA) for the apoptosis assay. NORAD knockdown and NC cells were harvested and resuspended ($5\times10^5$ cells per sample) before 5 μl of Annexin V-APC and 7-AAD were added to the suspensions and incubated for 15 minutes at room temperature in the dark. Flow cytometry was used to evaluate the luciferase intensity of Annexin V-APC and 7-AAD. A Cell Cycle Staining Kit (BD Pharmingen TM, New Jersey, USA) was used for evaluating the cell cycle distribution. Cells were fixed with 70% ethanol for 2 hours at 4°C. Target cells were treated with DNA staining solution and permeabilization solution in darkness for 15 minutes at room temperature. Flow cytometry was used to evaluate the luciferase intensity at 24 hours after treatment.

### 11. Replication fork recovery

Immunofluorescence assays of BrdU foci (BrdU in double-stranded DNA) were used to evaluate replication fork recovery after exposing ESCC cells to radiation [19, 20]. BrdU was incorporated into double-stranded DNA, and the immunofluorescence intensity of BrdU foci represented activation of replication fork recovery. Cells were exposed to 8 Gy of radiation before BrdU was added to the culture medium at a final concentration of 10 μM and incubated with the cells for 30 minutes. Cells with active replication forks were indicated by the cells with positive BrdU foci under a fluorescence microscope. Cells that did not receive radiation treatment were used as the control group.

### 12. Colony formation assay

Cells (500, 1000, 2000, 4000, or 8000 per well) were seeded into 6-well plates and cultured overnight in a 5% CO2 incubator before they were exposed to 0, 2, 4, 6, or 8 Gy of X-ray radiation. Colonies containing more than 50 cells were counted after 2 weeks of incubation. The survival curve after radiation was fitted based on the single-hit multitarget model: SF = 1 − (1 − e-D/D0)n.

### 13. Tandem mass tag proteomic-based quantitative proteome analysis

Cells successfully infected with lentivirus containing sh-NORAD or sh-NC were sonicated in lysis buffer (8 M urea, 1% Protease Inhibitor Cocktail) to extract total protein. The protein sample was pretreated with dithiothreitol, alkylated with iodoacetamide and diluted with TEAB. Then, the protein mixture was incubated with trypsin, desalted on a Strata X C18 SPE column (Phenomenex) and vacuum-dried. A tandem mass tag (TMT) kit was used for further labeling. The peptides were thereafter evaluated by tandem mass spectrometry (MS/MS) on a Q ExactiveTM Plus (Thermo) coupled to the UHPLC system.

The data-dependent procedure alternated between one MS scan followed by 20 MS/MS scans with 15.0 s dynamic exclusion and an automatic gain control (AGC) of 5E4. The fixed first mass was set as 100 m/z.

### 14. Xenograft mouse model and radiation treatment

ESCC cells suspended in phosphate-buffered saline were mixed with Matrigel and were injected into the right flanks of nude mice (KYSE-150 model, $5\times10^6$ cells) and C57BL/6 mice (AKR model, $1\times10^6$ cells). After the tumor volume reached 50-100 $mm^3$ in the KYSE-150 model and 150 $mm^3$ in the AKR model, local radiation (2 Gy/day for 4 consecutive days) was administered to the tumor site. Mice receiving concurrent treatment were also injected with anti-PD-1 antibody at 0, 7, and 14 days after the first radiation treatment. The tumor volume was measured with calipers and calculated using the following formula: tumor volume=0.5´ $width^2$ × length.

### 15. Whole exome sequencing

Agilent V6 Exon + UTR region probe was used. Primitive paired-end reads were screened to generate clean reads. Then BWA was used to compare the clean reads to H19 and rearrange the clean reads according to Karyotype by Picard. Then Samtools and Picard were used for redundancy removal. After that, GATK was used to generate the SNPs/INDELs variation information, which was annotated by VEP. Tumor mutation burden (TMB) was then calculated (TMB= total somatic mutations/total length of target region).

### 16. Statistical analysis

GraphPad Prism 8.2.1 and R 3.3.1 were used for statistical analysis and data visualization. Student's t test was performed to test differences between two groups, and one-way ANOVA was used to test differences among multiple groups. P□0.05 was considered statistically significant.

## Results

### 1. High NORAD expression indicates ESCC radioresistance.

To explore the NORAD's mechanism in ESCC radio-resistance, we established the acquired radioresistant ESCC cells (termed as KYSE-150R and TE-1R) as described in method 2. Colony formation assay confirmed that radioresistant ESCC cells were constructed successfully ( Fig.1A-D). The qRT-PCR results showed that NORAD expression was significantly upregulated in KYSE-150R and TE-1R cells compared with KYSE-150 and TE-1 cells (Fig. 2A). Following irradiation and other genotoxic agents (doxorubicin and cisplatin), NORAD expression was approximately 2~3-fold higher in ESCC cells (Fig. 2B). qRT-PCR and Immunofluorescence (IF) results confirmed that cytoplasmic NORAD but not nuclear NORAD were significantly increased in response to irradiation (Fig. 2C-E). FISH results from 77 ESCC patients who had been treated with definitive radiation indicated that NORAD was mainly expressed in the cytoplasm (Fig.

2F); thus, NORAD expression was subsequently examined in 41 ESCC tissues by qRT-PCR. High NORAD expression was associated with local recurrence after radiotherapy in ESCC patients (Fig. 2G-H). ROC curves indicated that NORAD can strongly predict local recurrence for ESCC patients who were treated with radiotherapy (Fig. 2I).

### 2. Irradiation activates NORAD expression via enhancing H3K4me2 enrichment

Histone H3 modifications of radioresistant ESCC cells and their parental cells were measured by using the EpiQuik™ Histone H3 Modification Multiplex Assay Kit. We observed that H3K4me3, H3K27me3 and H3k9ac were decreased while H3K4me2 showed increased expression in radioresistant ESCC cells ( Fig. 3A). By using genome bioinformatics analysis (http://genome.ucsc.edu/), we found that NORAD had high enrichment of H3K4me2 in MCF-7, HCT-116, SK-N-SH and KMS-11 cancer cells (Supplementary Fig. 1A). Western-blot analyses results showed a dynamic change of H3K4me following irradiation treatment, reaching a peak at 24 h (Fig. 3B). We next performed the ChIP assay in radioresistant ESCC cells and found that H3K4me2 was enriched at NORAD region. Notably, the enriched intensity of H3K4me2 was enhanced in radio-resistant cells compared with the parental cells (Fig. 3C). Based on TCGA datasets, we found the H3K4 methyltransferases, including Ash1, KMT2A, KMT2B, KMT2C, KMT2D, KMT2E, Set1A, Set1B, SETD7, SMYD2, SMYD3, WDR5 were positively correlated with NORAD expression (Supplementary Fig.1B). ESCC patients with KMT2B, KMT2C or KMT2D muted showed slightly lower NORAD expression but there was no statistic difference (Fig.3D). Knockdown ASHL2 (H3K4 methyltransferases) resulted in dereased H3K4me2 and NORAD expression(Fig.3E); and impairing the up-regulation of NORAD upon irradiation(Fig.3F). Together, these results showed that irradiation induced NORAD high expression were due to enhancing H3K4me2 enrichment at the NORAD region.

### 3. NORAD knockdown sensitizes ESCC to irradiation *in vitro and in vivo* by inhibiting homologous recombination repair

We next knockdown NORAD in KYSE-150R and TE-1R cells by lentivirus. Flow cytometry-based apoptosis assays demonstrated that NORAD knockdown alone increased the apoptosis rates of KYSE-150 and TE-1 cells and markedly increased the apoptosis rates in irradiated cells (Fig.4A-B). Xenograft tumor from NORAD knockdown and control cells showed that NORAD knockdown sensitized ESCC to radiation significantly in vivo (Fig.4C-D). BrdU immunofluorescence assays were adopted to measure replication fork restart after stalling upon DNA damage. Nascent DNA after DNA damage could be labeled with BrdU. Fewer BrdU-positive cells were observed in the NORAD knockdown group, suggesting that NORAD knockdown delayed the recovery of the stalled replication fork after radiation treatment (Fig. 4E-F). Regarding cell cycle distribution, NORAD knockdown arrested ESCC cells at G1 phase. We exposed ESCC cells to 8 Gy of radiation and found a significant increase in the number of cells arrested in G2 phase, whereas NORAD knockdown in combination with radiation attenuated G2 phase arrest (Fig. 4G-H). To determine if NORAD regulates DNA repair, recombination DR-GFP plasmids were transfected into cells with and without NORAD knockdown. DR–GFP plasmid-based HR assay showed that NORAD knockdown led to a 3~4-fold reduction in homologous recombination repair upon DSBs (Fig4.I-J).

### 4. NORAD knockdown-derived exosomes sensitizes ESCC cells to irradiation

We co-cultured NORAD knockdown cells with radioresistant ESCC cells, colony formation assay upon 2 Gy treatment results showed that NORAD knockdown not only sensitized cells themselves to radiation, but also sensitized KYSE-150R and TE-1R which were co-cultured with NORAD knockdown cells to radiation. It is notable that this inhibitory effect could be reversed by GW4869 (Fig.5A-B). We speculated that NORAD knockdown cells might affect co-cultured cells via exosomes. We then extracted exosomes from NORAD-knockdown cells, which were termed sh-NORAD exosomes. The extracellular vesicle-like structure of exosomes derived from sh-NORAD cells was confirmed by electron microscopy(Fig.5C); NTA (Nano Track Analysis) was also used to assess the particle size and relative number of particles in combination with CD63 expression to confirm their identity as exosomes (Fig. 5D-F). Exosome tracer experiments showed that sh-NORAD exosomes began to enter KYSE-150R and TE-1R cells after 6 hours of incubation and were enriched in the cytoplasm after 24 hours (Fig.5F). Decreased colony counts were observed as well for KYSE-150R and TE-1R cells treated with sh-NORAD exosomes in response to 2 Gy radiation (Fig.5G-H).

### 5. NORAD knockdown sensitizes co-cultured radioresistant ESCC cells to irradiation by promoting exosomal miR-199a-5p dismension.

Cancer-secreted exosomal miRNAs have been validated in numerous studies for regulating the crosstalk between cancer and stromal cells. We, therefore, investigated that whether NORAD regulated co-cultured cells via via exosomal miRNAs. We next performed the microRNA-sequence assay in exosomes of KYSE-150 and KYSE-150R. Top 30 differently expressed microRNAs are presented as heatmaps. 115 miRNAs were up-regulated and 56 miRNAs were down-regulated in sh-NORAD exosomes (Fig. 6A-D). We next examined Top5 miRNAs in NORAD knockdown cells (Fig. 6E). qRT-PCR results confirmed that miR-199a-5p was significantly overexpressed in sh-NORAD exosomes as well(Fig. 6F). To investigate whether exosomal miR-199a-5p could be delivered to the co-cultured cells,KY-SE150Rand TE-1R were cultured with the sh-NORAD cells or sh-NORAD exosomes. We found that co-incubation results in the increasion of miR-199a-5p inKY-SE150Rand TE-1R(Fig. 6G-H). Furtherly, we found that miR-199a-5p was down-regulated inKY-SE150Rand TE-1R when compared with parental control cells (Fig. 6I). miR-199a-5p was down-regulated in ESCC cells following irradiation treatment(Fig. 6J). Colony formation assay results confirmed that overexpression of miR-199a-5p sensitizedKY-SE150Rand TE-1R to irradiation(Fig.6K-L). These results might indicate that NORAD knockdown cells re-sensitize radio-resistance cells to irradiation via exosomal miR-199a-5p pathway.

### 6. NORAD inhibits pri-miR-199a process by competitively binding PUM1

No complementary sequence existed between miR-199a-5p and NORAD. CLIP-Seq data demonstrated that PUM1, which was regulated by NORAD, bound pri-miR-199a as well(Fig.7A). RIP-qPCR results confirmed the interaction of PUM1 with pri-miR-199a and NORAD respectively(Fig.7B). And NORAD knockdown enhanced the interaction between PUM1 and pri-miR-199a(Fig.7C). We speculated that whether NORAD regulated miR-199a-5p from PUM1. Western-blot showed that NORAD knockdown

increased the PUM1 expression. And radiation treatment decreased the PUM1 expression(Fig.7D). PUM1 knockdown significantly increased the pri-miR-199a expression but decreased the matural miR-199a-5p(Fig.7E-F). qRT-PCR result showed NORAD knockdown results the pri-miR-199a slightly decreasion which could be resuced by PUM1 knockdown(Fig.7G). Because miR-199a is not natively expressed in HEK293 cells, we knocked down PUM1 in HEK293 cells using siRNA and then overexpressed pri-miR-199a, which resulted in lower miR-199a-5p expression in PUM1-knockdown cells (Fig. 7H). We next constructed the overexpression plasmid of PUM1 or a PUM1 mutant lacking the RNA-binding domain (PUM1-mt). We found that pri-miR-199a was decreased in cells over-expressing PUM1 but not PUM1-mt; radiation increased the pir-miR-199a expression in cells over-expressing FLAG-PUM1, but not PUM1-mt(Fig.7I). Together, these results confirmed that NORAD delays the process of pri-miR-199a by competively binding PUM1.

### 7. NORAD knockdown impairs homologous recombination repair by down-regulating EEPD1.

To gain further insight into the potential proteins regulated by NORAD, we performed TMT mass spectrometry to quantify the protein levels in KYSE-150-sh-nc and KYSE-150-sh-NORAD cells (Supplementary Fig.2A-B). KEGG analysis of the downregulated protein in NORAD knockdown cells, demonstrating these proteins were enriched for nervous system disease such as huntington disease, parkinson disease, rheumatoid arthritis, cell cycle process, oxidative phosphorylation, immune system process and so on (Supplementary Fig.2C-D). Simutanously, starbase dataset was adopted to predicred the potential targets of miR-199a-5p. We found that EEPD1, the gatekeeper for repair of stressed replication forks, which was up-regulated in radio-resistant cells and significantly down-regulated in NORAD knockdown cells (Supplementary Fig.2E-F Fig.8A). IHC staining of xenograft tumors showed that tumors derived from NORAD-knockdown cells exhibited less EEPD1 staining (Fig.8B). EEPD1 w as downregulated after transducing radioresistant cells with miR-199a-5p mimics and upregulated after transducing normal control cells with miR-199a-5p inhibitors (Fig. 8C). miR-199a-5p mimics significantly decreased the relative luciferase activity of EEPD1-Wt but failed to influence the relative luciferase activity of EEPD1-Mut, indicating that miR-199a-5p interacts with the 3'UTR of EEPD1 mRNA (Fig. 8D). EEPD1 expression in 77 ESCC patients was further evaluated by IHC. EEPD1 is mainly expressed in the nucleus (Fig.8E). Among patients with radioresistant ESCC, 20 (20/29) showed high EEPD1 expression. The $c^2$ examination results showed that the radioresistance characteristic in ESCC was significantly associated with high EEPD1 expression ($\chi^2$=8.151; p=0.004**; Table 1). Based on TCGA datasets, we next identified radioresistance-related genes in ESCC by using random forest algorithm; the IncMSC and IncNodePurity values of EEPD1 were obviously higher than those of the other genes (Fig.8F). Furtherly, based on EEPD1 expression in TCGA datasets, the values of the area under the ROC curve (AUC) for segregating radio-resistant patients from radio-sensitive patients were 0.889 (95%CI 0.729-1.000) (Fig.8G). Xenograft tumor from EEPD1 knockdown and control cells showed that EEPD1 knockdown sensitized ESCC to radiation significantly in vitro and in vivo (Fig.8H). The HR reporter assay showed that EEPD1-knockdown cells presented lower HR rates after DNA double-strand breaks as well(Fig.8I). We found that EEPD1 knockdown inhibits the ATR and Chk1 phosphorylation upon irradiation treatment, which were consistent

with NORAD knockdown cells' phenotype(Fig.8J-K). And EEPD1 overexpression restored the phosphorylation of ATR-Chk1, which was reduced in NORAD-knockdown cells after 8 Gy MV X-rays treatment(Fig. 8L).

### 8. High NORAD expression predicts radio-immunotherapy failure in vivo.

Considering that irradiation leaded to the severe DNA damage in cells and NORAD knockdown increased the genomic instability under DNA damage, we reasoned that NORAD knockdown increased the tumor mutation burden (TMB) load in ESCC upon irradiation. Based on xenografts tumor model, we found that radiation or NORAD knockdown alone did not change the TMB. But NORAD knockdown combined radiotherapy increased the TMB load following radiation treatment (Fig.9A-C). Previous studies suggested that tumor mutational burden (TMB) may predict clinical response to immune checkpoint inhibitor, we investigated if NORAD knockdown combined with radiation enhanced the anti-PD-1 efficiency on C57BL/6 mice. AKR-radioresistant cells were construced by exposing cells to 2 Gy irradiation every 2 days(termed as AKR-R).We found that Anti-PD-1 monotherapy was not enough for controlling the tumor growth. In combination therapy group, we found that radiotherapy combined with anti-PD-1 therapy suppressed the tumor growth efficiently only in NORAD knockdown group but not control group. (Fig.9D-E). We next examined PD-L1 expression in NORAD-knockdown cells. NORAD-knockdown cells displayed elevated PD-L1 protein expression (Fig. 9F), and IHC staining of xenograft tumors showed that tumors derived from NORAD-knockdown cells exhibited stronger PD-L1 staining (Fig. 9G) than did tumors derived from control cells. We treated cells with the proteasome inhibitor MG132 and subsequently Co-IP experiments indicated that the levels of PD-L1 ubiquitination was elevated in radioresistant ESCC cells. NORAD knockdown impaired PD-L1 ubiquitination (Fig9.H). These results demonstrated that NORAD inhibits ubiquitination of PD-L1. By subsequently evaluating the tumor infiltrating lymphocyte, however, we did not find significantly change for tumor infiltrating lymphocyte between NORAD knockdown mice group and control group(Supplementary Fig.3A). Based on CIBERSORT, we found that NORAD expression did not affect the immune cell infiltration either(Supplementary Fig.3B). It is demonstrated that NORAD influenced the immunogenic function of radiation but not the tumor immune microenvironment. Taken together, these results uncover that NORAD is a potential treatment target for improving the efficacy of immunotherapy in ESCC patients.

## Discussion

Previously, our group identified that lncRNA-NORAD, whose expression is induced by DNA damage, plays key roles in mediating radiation resistance. NORAD is overexpressed in ESCC both in vivo and in vitro; furthermore, NORAD knockdown sensitizes ESCC cells to radiation treatment. In this manuscript, we further investigated the corresponding molecular mechanisms. NORAD delays pri-miR-199a maturation by inhibiting the interaction of PUM1 with pri-miR-199a and subsequently releasing EEPD1, which can be recruited to damaged DNA and promote HR in response to radiation. Concurrently, NORAD knockdown inhibits PD-L1 ubiquitination and enhances anti-PD-1 treatment efficacy, especially in combination with

radiotherapy. Our results indicate that NORAD acts as a novel target for improving the efficacy of radiation and anti-PD1 therapy by regulating the DNA damage response.

The HR-reported assay results confirm that NORAD knockdown sensitizes ESCC to radiation by inhibiting HR efficiency. We subsequently confirmed that NORAD knockdown delays the HR process by inhibiting ATR/Chk1 signaling activation in response to radiation. Evidence has suggested that inhibiting DNA repair components, including ATM, ATR, Chk1 and Chk2, markedly sensitizes cancer cells to radiation[23-25]. For example, Teng et al found that inhibiting either ATM or ATR significantly enhanced the radiation response in gynecological cancer cells (ovarian, endometrial, and cervical cancer cells) [26]. Notably, the generation of double-strand breaks is the central mechanism of action of radiotherapy. In response to radiation-induced DNA damage, ATM, ATR and DNA-$PK_S$, three important DNA damage sensors, are immediately activated and arget a variety of overlapping substrates that promote DNA repair, cell cycle arrest and apoptosis[27, 28]; these biological processes help cancer cells escape radiation damage. We found that under radiation stress, NORAD knockdown significantly increased ESCC apoptosis rates and impaired arrest at G2 phase, leading to genomic instabilities in ESCC cells. Based on these results, we inferred that NORAD is an effecitve target for enhancing the cytotoxic effects of radiation in ESCC.

Two major mechanisms have been reported with regard to NORAD-mediated regulation of genomic stability. A recent study revealed that NORAD acts as an RNA-binding protein; interacts with RBMX, TOP1 and other proteins; and facilitates the formation of the topoisomerase complex[11]. An earlier study confirmed that NORAD maintained genomic stability by binding to and negatively regulating PUMILIO (PUM1 and PUM2) in the cytoplasm[10, 29]. To explore how NORAD regulates ATR signaling activation in response to radiation, we performed TMT mass spectrometry to identify the NORAD-regulated proteins. The KEGG and GO analyses of differentially expressed proteins revealed that the biological processes mainly focused on DNA metabolic process, cell cycle, immune stimulation and so on. Consistently, we confirmed the interaction between NORAD and PUM1 and found that NORAD knockdown significantly upregulated PUM1 expression.

As an RNA-binding protein, PUM1 binds to RNAs containing the PUMILIO response element (UGUANAUA or UGUANAUN), thus mediating RNA deadenylation, decapping, and degradation[29]. In this study, we found that PUM1 can bind pri-miR-199a and facilitate the Drosha processing of pri-miR-199a. miRNAs are transcribed initially as pri-miRNAs and recognized by RNase III DROSHA and RNA-binding protein DGCR8 in the nucleus. The flanking single-stranded sequences are cleaved by DROSHA and generate pre-miRNAs, which are then cleaved by the RNase III Dicer to generate double-stranded RNA ~21 nucleotides (nt) in length. Recently, numerous studies have reported that the expression level of mature miRNA is driven by both transcription and processing rates during the Drosha and Dicer processes[30]. For example, Guil et al stated that hnRNP A1, an RNA-binding protein, specifically bound to pri-miR-18a before the Drosha process[31]. Another stem cell factor, LIN28, interacted with pre-miRNAs of the let-7 family and recruited uridyltransferases to these pre-miRNAs, essentially blocking their expression[32]. Here, we found that PUM1 can bind to pri-miR-199a and function as an auxiliary factor for the pri-miR-199a Drosha process. This interaction could be inhibited by NORAD, as upregulation of NORAD significantly

delays the Drosha process of pri-miR-199a by sequestering PUM1 in the cytoplasm. Notably, NORAD knockdown not only facilitates the processing of miR-199a-5p by inhibiting PUM1 but also restores the radiosensitivity of cocultured radioresistant ESCC cells. NORAD knockdown drives the transfer of exosomal miR-199a-5p from NORAD-knockdown cells to radioresistant cells. In addition, EEPD1 was downregulated in radioresistant ESCC cells. Taken together, these results expanded the potential clinical importance of NORAD in ESCC radiotherapy.

With the assistance of WGCNA and randomForest, we identified the target genes of miR-199a-5p and EEPD1. Dual-luciferase reporter assays validated the direct interaction of EEPD1 and miR-199a-5p. Based on the IHC results, we observed that EEPD1 is a powerful biomarker for predicting the radioresistance of ESCC. Wu et al previously reported that EEPD1 can be recruited to stalled forks in response to DNA damage, where it promotes the restarting of these stalled forks by resecting the 5' DNA end near the fork junction, thus permitting the invasion of the 3' single strand and the initiation of HR[33]. Hyun-Suk Kim et al stated that EEPD1 acts as a gatekeeper for HR; it cleaves replication forks and creates a binding site for Exo1 on the free 5' DNA end[19]. Furthermore, Changzoon Chun et al reported that the biological function of EEPD1 is similar to that of BRCA1. Depletion of EEPD1 in stressed zebrafish embryos results in chromosomal abnormalities, including anaphase bridges and micronuclei[34]. These results confirm that EEPD1 functions at the initiation of HR and that deleting EEPD1 sensitizes cells to DNA replication stressors.

Interestingly, we found that NORAD knockdown also enhances the efficacy of immune checkpoint inhibitors in combination with radiotherapy in tumor treatment. NORAD knockdown upregulates PD-L1 expression by inhibiting its ubiquitination. These phenomena may suggest the poor response of radioresistant ESCC patients to immune checkpoint inhibitors. One study found that PD-L1 protein expression fluctuated during the cell cycle and peaked at G1 phase. Researchers have reported that PD-L1 is regulated by the G1 cycle checkpoint Cyclin D-CDK4 via the Cullin3$^{SPOP}$-E3 ligase pathway[35]. Here, we found that NORAD knockdown induces ESCC cell arrest in the G1 cell cycle, which might be responsible for the observed PD-L1 upregulation. In ESCC patients, only a limited number of patients could benefit from anti-PD1 therapy. In the last prospective clinical trial, pembrolizumab did not improve overall survival compared with paclitaxel as a second-line therapy for advanced esophageal cancer[36]. Radiation both alone and in combination with anti-PD-1 treatment suppressed tumor growth, but the combination did not significantly improve the tumor response compared to that of radiation monotherapy. For mice bearing AKR-sh-NORAD tumors, the use of combination therapy significantly inhibited tumor growth compared with that in response to radiation monotherapy. It is worth noting that NORAD knockdown significantly facilitates the antitumor efficiency of anti-PD-1 and radiation in ESCC. These results uncover that NORAD is a potential treatment target for improving immunotherapy efficacy in ESCC patients. conceptually, inhibiting DNA damage repair can augment the efficacy of radiotherapy in combination with immune checkpoint inhibitors in ESCC.

# Abbreviations

EAC: Esophageal Adenocarcinoma

ESCC: Esophageal Squamous Cell Carcinoma

TMT Mass Spectrometry: Tandem Mass Tag Mass Spectrometry

HR: Homologous Recombination

NEJM: Non-homologous End Joining (NHEJ)

DR-GFP: Reporter Direct Repeat - Green Fluorescent Protein Reporter

NTA: Nano Track Analysis

WGCNA: Weighted Gene Co-Expression Network Analysis

KEGG: Kyoto Encyclopedia of Genes and Genomes

GO: Gene Ontology

STRING: Search Tool for the Retrieval of Interacting Genes/Protein

IncMSC: Increase in MSE

IncNodePurity: Increase in NodePurityxs

# Declarations

### Ethics approval and consent to participate

This study was approved by the Ethics Committee of the First Affiliated Hospital of Xi`an Jiaotong University.

### Consent for publication

All authors have agreed to the publication of this research.

### Availability of data and materials

Data and materials are available upon reasonable request if applicable.

### Competing interests

The authors declare no conflicts of interest.

### Funding

This research was funded by the National Natural Science Foundation of China (grant number 81773239).

### Authors' contributions

Sun Yuchen Sun and Wang Jizhao designed and conducted the experiments, wrote the manuscript and prepared the figures. Cai Hui and Li Jing conducted the animal experiments and assisted in the in vitro experiments. Sun Xuanzi assisted in the execution of the in vitro experiments and preparation of the figures. Su Yani assisted in the execution of the in vitro experiments. Shi Xiaobo and Zhao Xu assisted in formatting the manuscript and figures. Zhang Xiaozhi sponsored, conceived of, and supervised the study.

### Acknowledgments

Not applicable

## References

1. Bray F, Ferlay J, Soerjomataram I, Siegel RL, Torre LA, Jemal A: **Global cancer statistics 2018: GLOBOCAN estimates of incidence and mortality worldwide for 36 cancers in 185 countries**. *CA Cancer J Clin* 2018, **68**(6):394-424.
2. Kitagawa Y, Uno T, Oyama T, Kato K, Kato H, Kawakubo H, Kawamura O, Kusano M, Kuwano H, Takeuchi H *et al*: **Esophageal cancer practice guidelines 2017 edited by the Japan Esophageal Society: part 1**. *Esophagus* 2019, **16**(1):1-24.
3. Huang FL, Yu SJ: **Esophageal cancer: Risk factors, genetic association, and treatment**. *Asian J Surg* 2018, **41**(3):210-215.
4. Kitagawa Y, Uno T, Oyama T, Kato K, Kato H, Kawakubo H, Kawamura O, Kusano M, Kuwano H, Takeuchi H *et al*: **Esophageal cancer practice guidelines 2017 edited by the Japan esophageal society: part 2**. *Esophagus* 2019, **16**(1):25-43.
5. Vaghjiani RG, Molena D: **Surgical management of esophageal cancer**. *Chin Clin Oncol* 2017, **6**(5):47.
6. Lagergren J, Smyth E, Cunningham D, Lagergren P: **Oesophageal cancer**. *Lancet* 2017, **390**(10110):2383-2396.
7. Chen GZ, Zhu HC, Dai WS, Zeng XN, Luo JH, Sun XC: **The mechanisms of radioresistance in esophageal squamous cell carcinoma and current strategies in radiosensitivity**. *J Thorac Dis* 2017, **9**(3):849-859.
8. Qian X, Tan C, Yang B, Wang F, Ge Y, Guan Z, Cai J: **Astaxanthin increases radiosensitivity in esophageal squamous cell carcinoma through inducing apoptosis and G2/M arrest**. *Dis Esophagus* 2017, **30**(6):1-7.
9. Fatica A, Bozzoni I: **Long non-coding RNAs: new players in cell differentiation and development**. *Nat Rev Genet* 2014, **15**(1):7-21.

10. Lee S, Kopp F, Chang TC, Sataluri A, Chen B, Sivakumar S, Yu H, Xie Y, Mendell JT: **Noncoding RNA NORAD Regulates Genomic Stability by Sequestering PUMILIO Proteins**. *Cell* 2016, **164**(1-2):69-80.
11. Munschauer M, Nguyen CT, Sirokman K, Hartigan CR, Hogstrom L, Engreitz JM, Ulirsch JC, Fulco CP, Subramanian V, Chen J *et al*: **The NORAD lncRNA assembles a topoisomerase complex critical for genome stability**. *Nature* 2018, **561**(7721):132-136.
12. Huang Q, Xing S, Peng A, Yu Z: **NORAD accelerates chemo-resistance of non-small-cell lung cancer via targeting at miR-129-1-3p/SOX4 axis**. *Biosci Rep* 2020, **40**(1).
13. Hu B, Cai H, Zheng R, Yang S, Zhou Z, Tu J: **Long non-coding RNA 657 suppresses hepatocellular carcinoma cell growth by acting as a molecular sponge of miR-106a-5p to regulate PTEN expression**. *Int J Biochem Cell Biol* 2017, **92**:34-42.
14. Czarny P, Wigner P, Galecki P, Sliwinski T: **The interplay between inflammation, oxidative stress, DNA damage, DNA repair and mitochondrial dysfunction in depression**. *Prog Neuropsychopharmacol Biol Psychiatry* 2018, **80**(Pt C):309-321.
15. Roos WP, Thomas AD, Kaina B: **DNA damage and the balance between survival and death in cancer biology**. *Nature reviews Cancer* 2016, **16**(1):20-33.
16. Santivasi WL, Xia F: **Ionizing radiation-induced DNA damage, response, and repair**. *Antioxid Redox Signal* 2014, **21**(2):251-259.
17. Vendetti FP, Karukonda P, Clump DA, Teo T, Lalonde R, Nugent K, Ballew M, Kiesel BF, Beumer JH, Sarkar SN *et al*: **ATR kinase inhibitor AZD6738 potentiates CD8+ T cell-dependent antitumor activity following radiation**. *J Clin Invest* 2018, **128**(9):3926-3940.
18. Sato H, Niimi A, Yasuhara T, Permata TBM, Hagiwara Y, Isono M, Nuryadi E, Sekine R, Oike T, Kakoti S *et al*: **DNA double-strand break repair pathway regulates PD-L1 expression in cancer cells**. *Nat Commun* 2017, **8**(1):1751.
19. Kim HS, Nickoloff JA, Wu Y, Williamson EA, Sidhu GS, Reinert BL, Jaiswal AS, Srinivasan G, Patel B, Kong K *et al*: **Endonuclease EEPD1 Is a Gatekeeper for Repair of Stressed Replication Forks**. *J Biol Chem* 2017, **292**(7):2795-2804.
20. Nimonkar AV, Genschel J, Kinoshita E, Polaczek P, Campbell JL, Wyman C, Modrich P, Kowalczykowski SC: **BLM-DNA2-RPA-MRN and EXO1-BLM-RPA-MRN constitute two DNA end resection machineries for human DNA break repair**. *Genes & development* 2011, **25**(4):350-362.
21. Schwartz JC, Cech TR, Parker RR: **Biochemical Properties and Biological Functions of FET Proteins**. *Annu Rev Biochem* 2015, **84**:355-379.
22. Mastrocola AS, Kim SH, Trinh AT, Rodenkirch LA, Tibbetts RS: **The RNA-binding protein fused in sarcoma (FUS) functions downstream of poly(ADP-ribose) polymerase (PARP) in response to DNA damage**. *J Biol Chem* 2013, **288**(34):24731-24741.
23. Ahmed M, Li L, Pinnix C, Dabaja B, Nomie K, Lam L, Wang M: **ATM mutation and radiosensitivity: An opportunity in the therapy of mantle cell lymphoma**. *Crit Rev Oncol Hematol* 2016, **107**:14-19.
24. Andreassen CN, Rosenstein BS, Kerns SL, Ostrer H, De Ruysscher D, Cesaretti JA, Barnett GC, Dunning AM, Dorling L, West CML *et al*: **Individual patient data meta-analysis shows a significant association**

**between the ATM rs1801516 SNP and toxicity after radiotherapy in 5456 breast and prostate cancer patients**. *Radiother Oncol* 2016, **121**(3):431-439.

25. Li MY, Liu JQ, Chen DP, Li ZY, Qi B, He L, Yu Y, Yin WJ, Wang MY, Lin L: **Radiotherapy induces cell cycle arrest and cell apoptosis in nasopharyngeal carcinoma via the ATM and Smad pathways**. *Cancer Biol Ther* 2017, **18**(9):681-693.
26. Teng PN, Bateman NW, Darcy KM, Hamilton CA, Maxwell GL, Bakkenist CJ, Conrads TP: **Pharmacologic inhibition of ATR and ATM offers clinically important distinctions to enhancing platinum or radiation response in ovarian, endometrial, and cervical cancer cells**. *Gynecol Oncol* 2015, **136**(3):554-561.
27. Jin MH, Oh DY: **ATM in DNA repair in cancer**. *Pharmacol Ther* 2019, **203**:107391.
28. Cimprich KA, Cortez D: **ATR: an essential regulator of genome integrity**. *Nat Rev Mol Cell Biol* 2008, **9**(8):616-627.
29. Elguindy MM, Kopp F, Goodarzi M, Rehfeld F, Thomas A, Chang TC, Mendell JT: **PUMILIO, but not RBMX, binding is required for regulation of genomic stability by noncoding RNA NORAD**. *Elife* 2019, **8**.
30. Dueck A, Meister G: **Assembly and function of small RNA - argonaute protein complexes**. *Biol Chem* 2014, **395**(6):611-629.
31. Guil S, Caceres JF: **The multifunctional RNA-binding protein hnRNP A1 is required for processing of miR-18a**. *Nat Struct Mol Biol* 2007, **14**(7):591-596.
32. Chang HM, Triboulet R, Thornton JE, Gregory RI: **A role for the Perlman syndrome exonuclease Dis3l2 in the Lin28-let-7 pathway**. *Nature* 2013, **497**(7448):244-248.
33. Wu Y, Lee SH, Williamson EA, Reinert BL, Cho JH, Xia F, Jaiswal AS, Srinivasan G, Patel B, Brantley A *et al*: **EEPD1 Rescues Stressed Replication Forks and Maintains Genome Stability by Promoting End Resection and Homologous Recombination Repair**. *PLoS Genet* 2015, **11**(12):e1005675.
34. Chun C, Wu Y, Lee SH, Williamson EA, Reinert BL, Jaiswal AS, Nickoloff JA, Hromas RA: **The homologous recombination component EEPD1 is required for genome stability in response to developmental stress of vertebrate embryogenesis**. *Cell Cycle* 2016, **15**(7):957-962.
35. Zhang J, Bu X, Wang H, Zhu Y, Geng Y, Nihira NT, Tan Y, Ci Y, Wu F, Dai X *et al*: **Cyclin D-CDK4 kinase destabilizes PD-L1 via cullin 3-SPOP to control cancer immune surveillance**. *Nature* 2018, **553**(7686):91-95.
36. Shitara K, Ozguroglu M, Bang YJ, Di Bartolomeo M, Mandala M, Ryu MH, Fornaro L, Olesinski T, Caglevic C, Chung HC *et al*: **Pembrolizumab versus paclitaxel for previously treated, advanced gastric or gastro-oesophageal junction cancer (KEYNOTE-061): a randomised, open-label, controlled, phase 3 trial**. *Lancet* 2018, **392**(10142):123-133.

# Table

Table 1. The correlation between EEPD1 expression and radiotherapy outcome in ESCC patients.

| | Radio-resistance | Radio-sensitive | Total | $\chi^2$ | P value |
|---|---|---|---|---|---|
| High expression | 20 | 17 | 53 | | |
| Low expression | 9 | 31 | 14 | 8.151 | 0.004** |
| Total | 29 | 48 | 77 | | |

# Figures

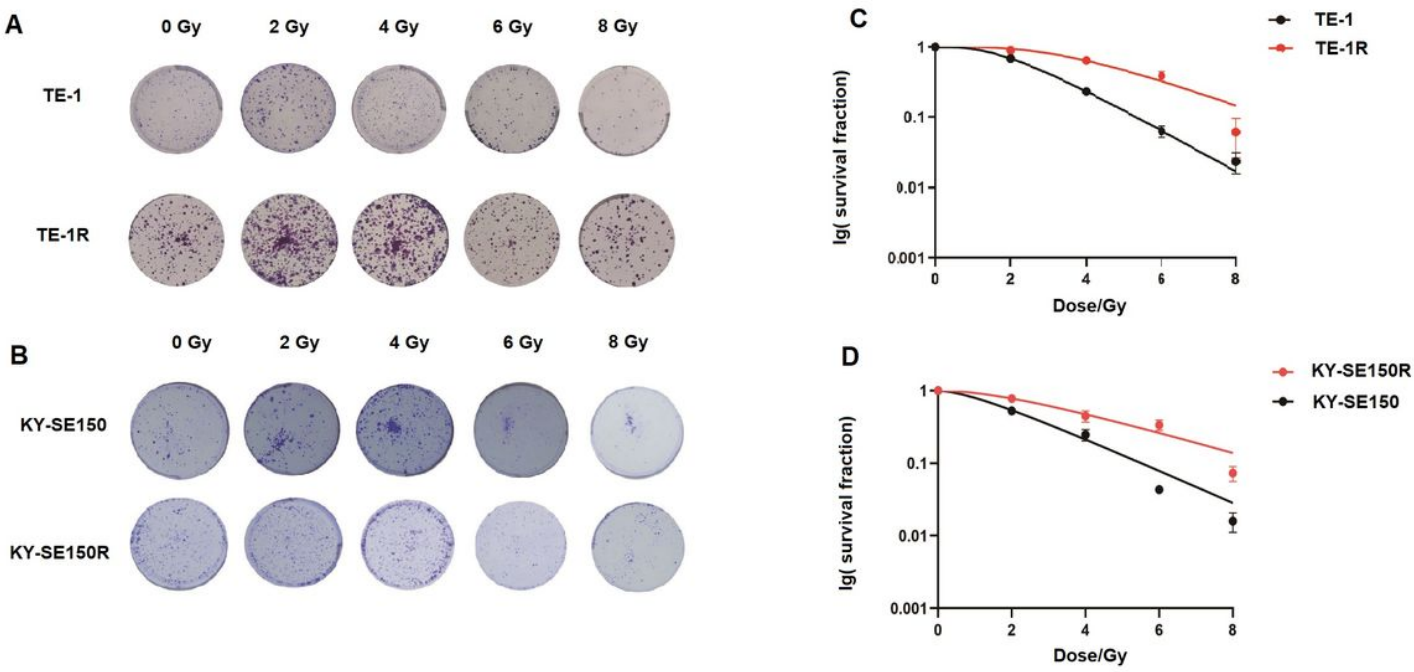


## Figure 1

A-B. Colony formation assay of TE-1, TE-1R and KYSE-150, KYSE-150R under 0, 2, 4, 6, 8 Gy MV X-rays. C-D. Dose survival curve of TE-1, TE-1R and KYSE-150, KYSE-150R cells on colony formation assay results.

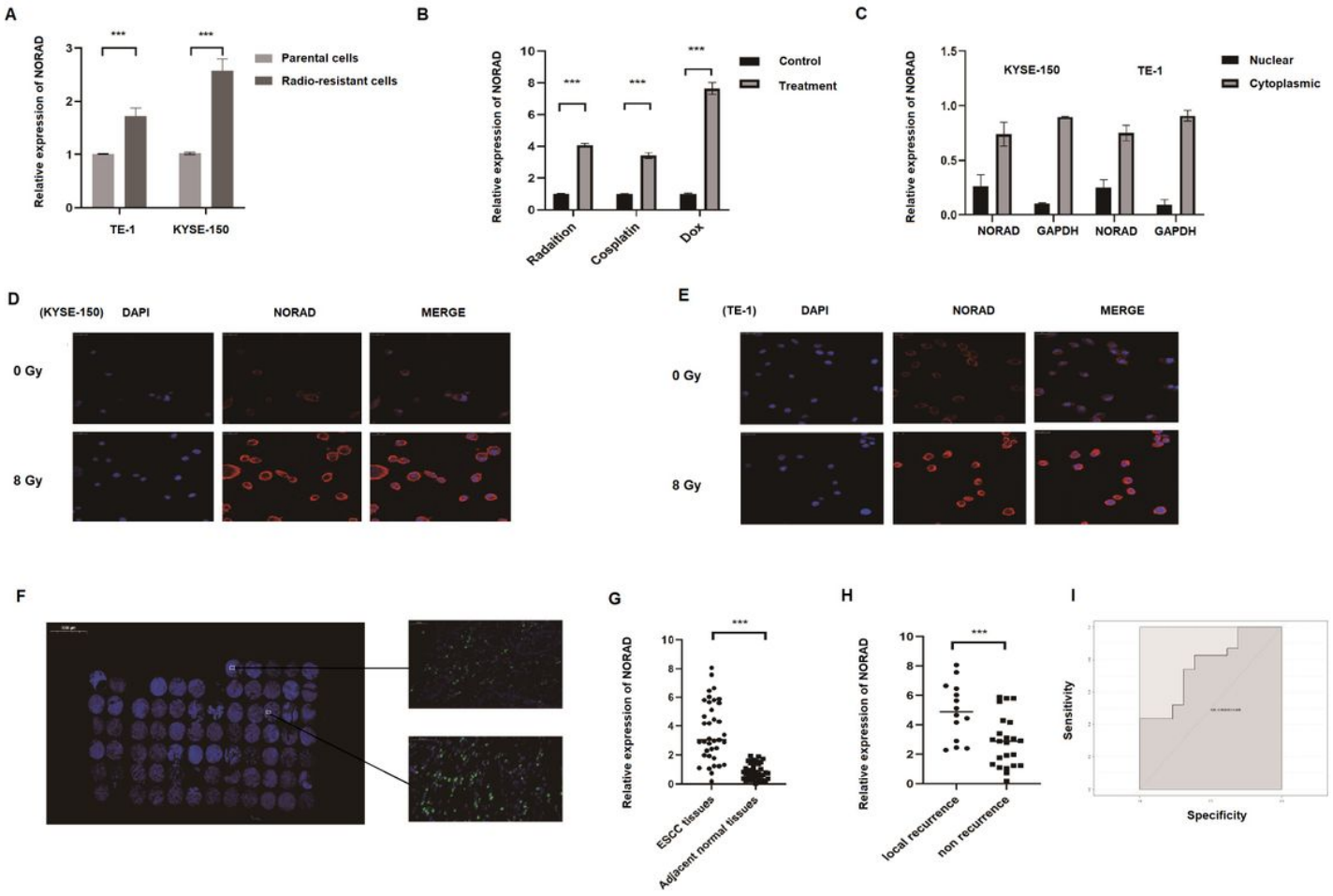


## Figure 2

A. qRT-PCR measurement of the NORAD expression in radio-resistant ESCC cells (KYSE-150R and TE-1R) and their parental cells (KYSE-150 and TE-1). B. qRT-PCR measurement of the NORAD expression in KYSE-150, which are treated with 8Gy MV X-rays, cisplatin and doxorubicin respectively. C. qRT-PCR measurement of subcellular fractionation of NORAD in KYSE-150 and TE-1 cells. (GAPDH is taken as cytoplasmic control). D-E. FISH result of NORAD expression in KYSE-150(D) and TE-1 (E) before and after 8 Gy MV X-rays treatment. F. Fluorescence images of RNA FISH showed the cytoplasmic distribution of NORAD in ESCC tissues. The scale bar represented 50 μm. G. qRT-PCR measurement of the NROAD expression in ESCC tissues and adjacent normal tissues. H. qRT-PCR measurement of the NROAD expression in ESCC tissues with local recurrence and non-recurrence. I. ROC curve for predicting ESCC local recurrence based on NORAD expression. AUC=0.763 (0.601-0.924; $p<0.05$).

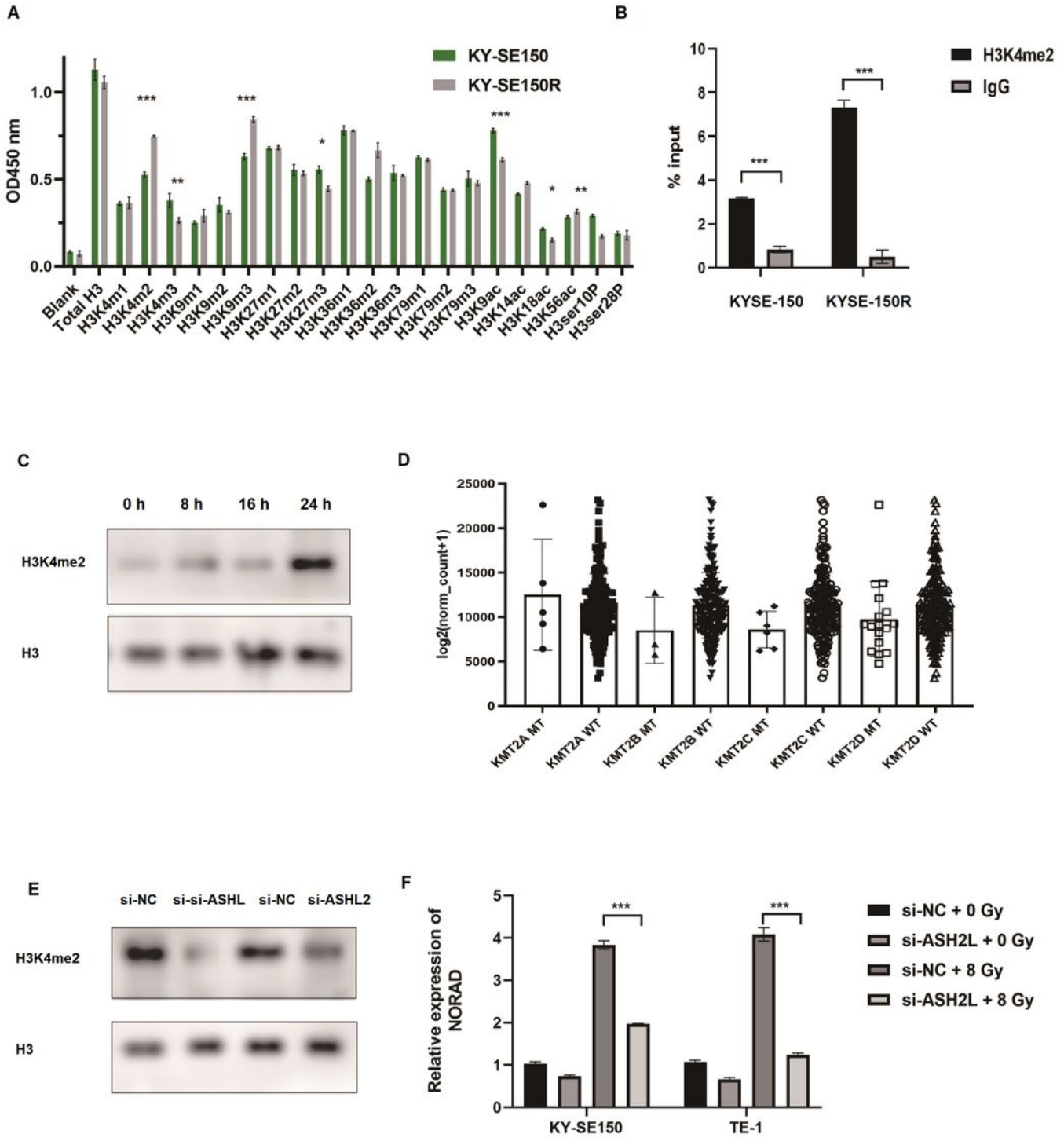


## Figure 3

A. 21 histone H3 modification of KYSE-150R and KYSE-150 cells. 100 ng of total histone proteins per well were used. B. The ChIP assay was performed to determine the enrichment of H3K4me2 of the NORAD region in KYSE-150 and KYSE-150R cells. C. The expression level of H3K4me2 measured in KYSE-150 cells at 6, 8, 16 and 24 h post-irradiation. Histone H3 was measured as a loading control. D. The expression level of NORAD in ESCC patients with KMT2B, KMT2C or KMT2D muted or wild type based on

TCGA datasets. E. The expression level of H3K4me2 measured by western blot with or without ASHL2 knockdown. F. qRT-PCR measurement of the NROAD expression in KYSE-150 and TE-1 cells with or without ASHL2 knockdown, which were treated with 8 Gy MV X-rays treatment.

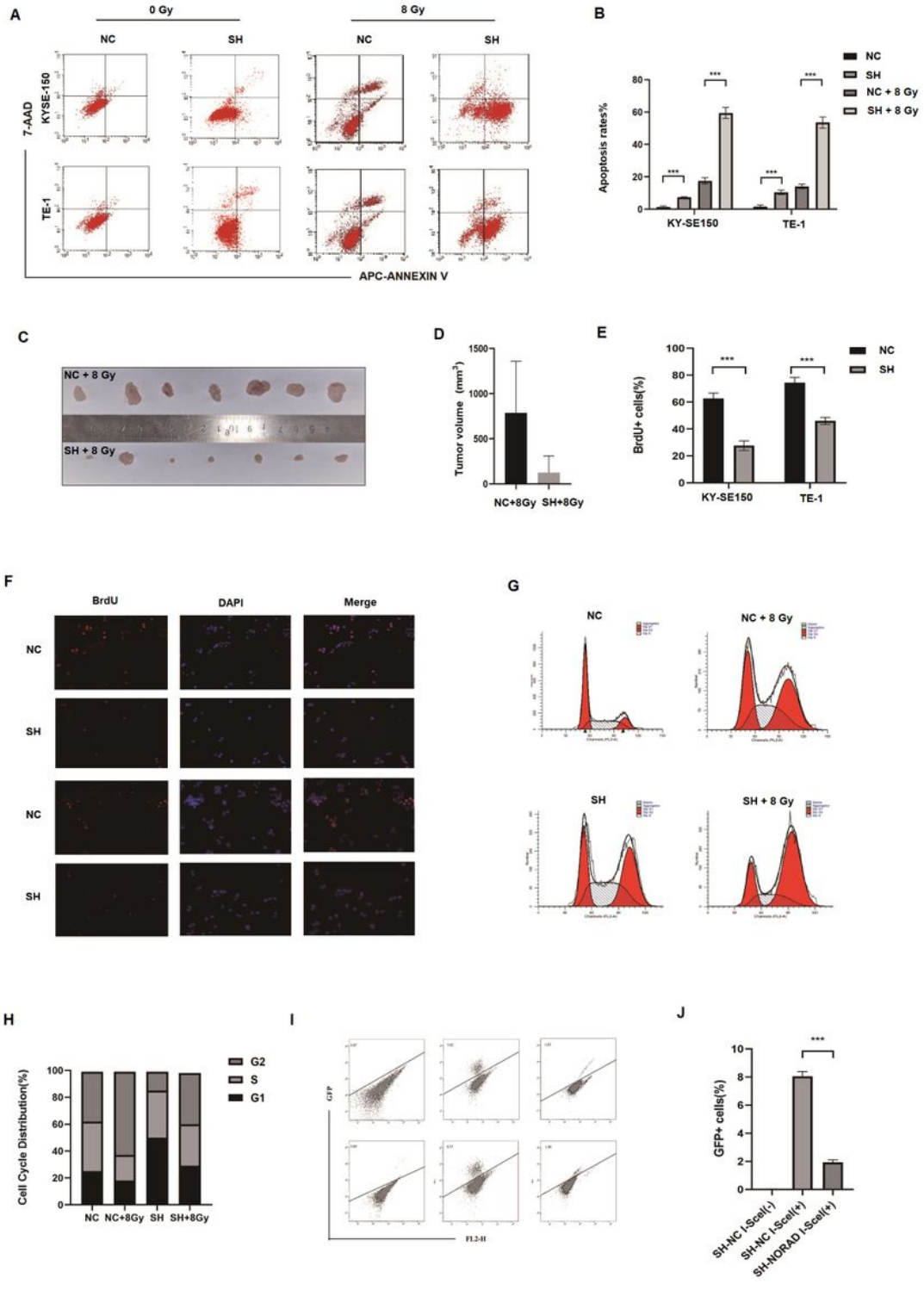


## Figure 4

A-B. A.The apoptosis of NORAD knockdown cells and control cells with or without irradiation treatment were measured by flow cytometry (Annexin V-APC/7-AAD double-staining assay); B. Quantification and

statistical analyses. C-D. C. The effect of NORAD on ESCC radio-sensitivity in ESCC xenografts. Subcutaneous ESCC xenografts were established with 1×106 SH-NORAD cells and 1×106 SH-NC cells respectively. The tumors were harvested and pictured at 18 days after radiotherapy delivery; D. Quantification of tumor volume in Fig.6P. (*P<0.05; mean ± S.E.M. were shown) E-F. E. Quantification and statistical analyses. F. Replication recovery assay for NORAD knockdown and control cells as percentage with positive BrdU foci after 8 Gy MV X-rays treatment; E. Quantification and statistical analyses. G-H. G.Cell cycle were evaluated by flow cytometry in NORAD knock down and control cells, with or without 8 Gy MV X-rays treatment. H. Quantification and statistical analyses. I-J. I. KYSE-150 and TE-1 are transfected with an I-SceI expression plasmid, HRR in NORAD knockdown cells and control cells are assayed by flow cytometry, and represented with the percent GFP positive cells. J. Quantification and statistical analyses.

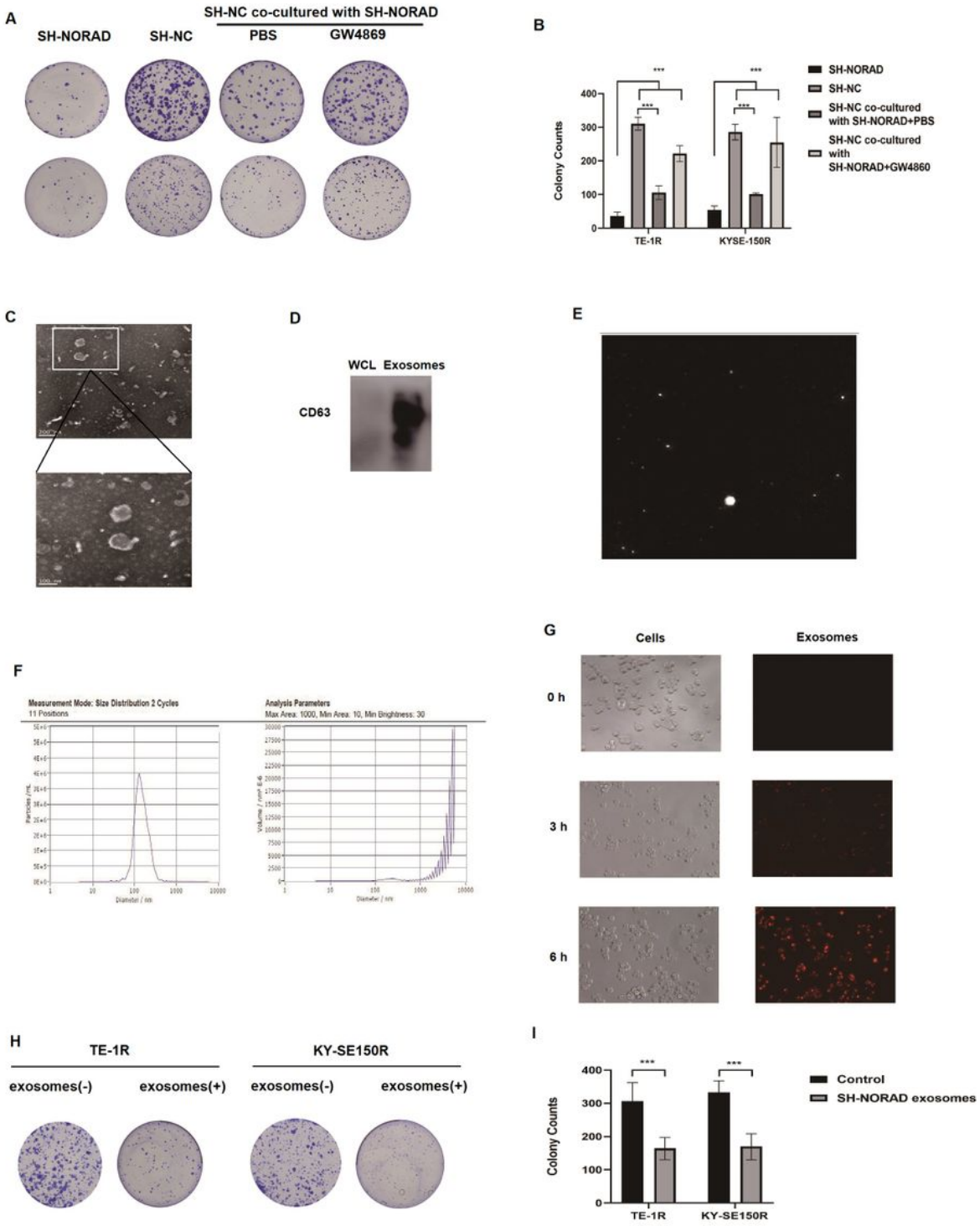


## Figure 5

A-B. A. Colony formation of KYSE-150R and TE-1R cells which were co-cultured with NORAD knockdown radio-resistant cells. All cells were exposed to 2 Gy MV X-rays on the second day after cells seeded into 6-well plates. B. Colony counts were quantified and shown Fig5.B C. Electron microscopy to confirm the exosomes extracted. D. Western blot to evaluate the exosome markers, CD63 in extracted exosomes. E. NTA (Nano Track Analysis) exosomes imaging with representative picture of exosomes. F. NTA was used

to assess the particle size and relative number of particles of exosomes extracted. G. Exosome tracer experiments to evaluate the ability of exosomes that entering target cells. H-I. Colony formation assay of KYSE-150R and TE-1R cells treated with or without sh-NORAD exosomes under 2 Gy MV X-rays. I. Colony counts were quantified.

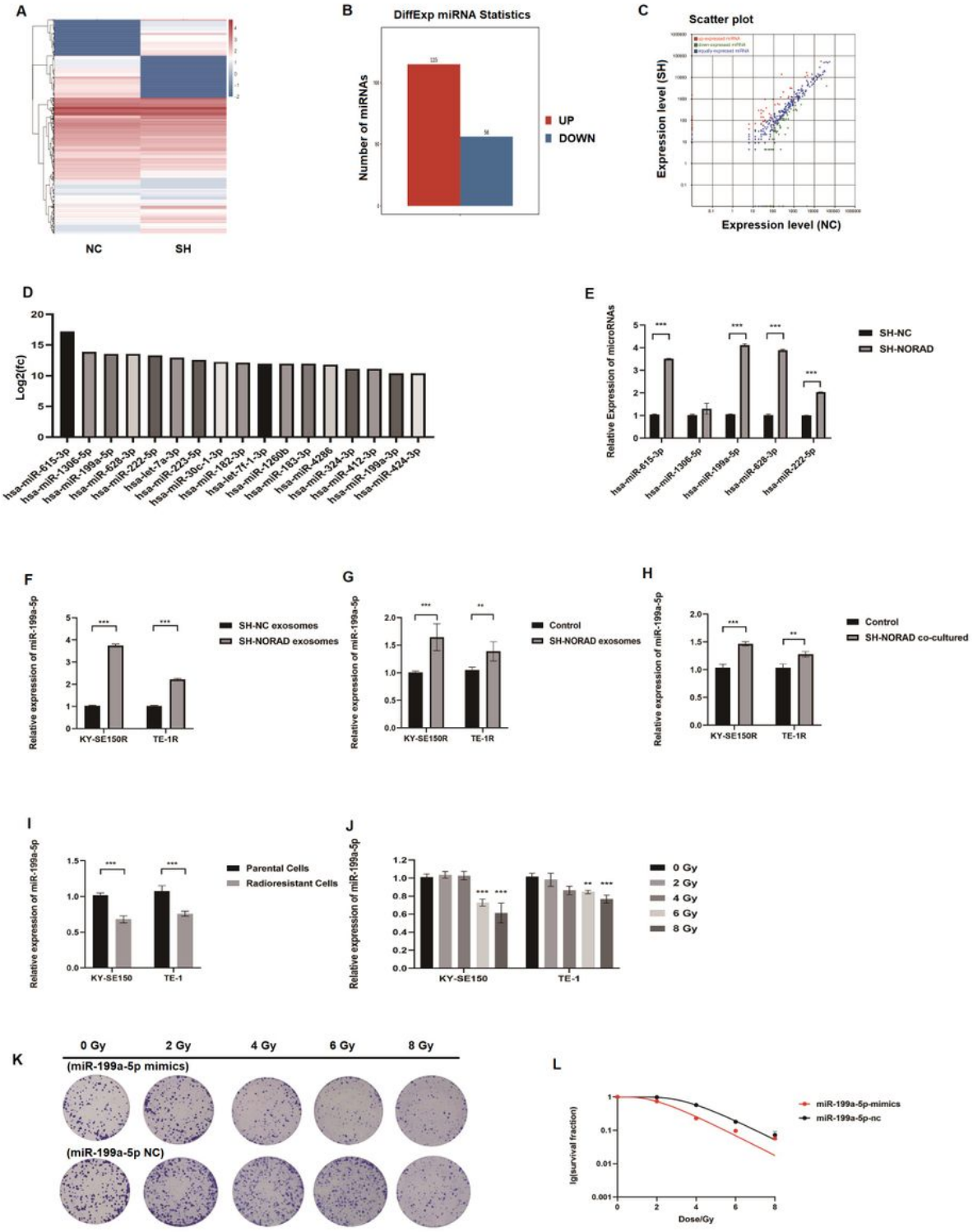


## Figure 6

A. Heatmap for top30 differentially expressed microRNAs between SH-NC exosomes and SH-NORAD exosomes. B. The numbers of up or down regulated microRNAs in SH-NORAD exosomes when compared with SH-NC exosomes. C. The individual expression scatter plot of microRNAs in SH-NC exosomes and SH-NORAD exosomes. D. Top 17 different expression microRNAs between SH-NC exosomes and SH-NORAD exosomes. Columns represent the Log2(FC) of two biological experiments. E. qRT-PCR to evaluate top 5 different expressed microRNAs in KYSE-150 cells with or without NORAD knockdown. F. qRT-PCR to evaluate the expression of miR-199a-5p in SH-NC exosomes and SH-NORAD exosomes. G. qRT-PCR to evaluate the expression of miR-199a-5p in radioresistant cells which were treated with SH-NORAD exosomes or not. H. qRT-PCR to evaluate the expression of miR-199a-5p in radioresistant cells which were co-cultured with NORAD knockdown cells or control cells. I. qRT-PCR to evaluate the expression of miR-199a-5p in radio-resistant ESCC cells (KYSE-150R and TE-1R) and their parental cells (KYSE-150 and TE-1). J. qRT-PCR to evaluate the expression of miR-199a-5p in KYSE-150 and TE-1 under 0, 2, 4, 6, 8 Gy MV X-rays treatment. K-L. Colony formation assay of KYSE-150 cells transfected with miR-199a-NC or miR-199a-mimics under 0, 2, 4, 6, 8 Gy MV X-rays. L. Dose survival curve of KYSE-150 cells transfected with miR-199a-NC or miR-199a-mimics on colony formation assay results.

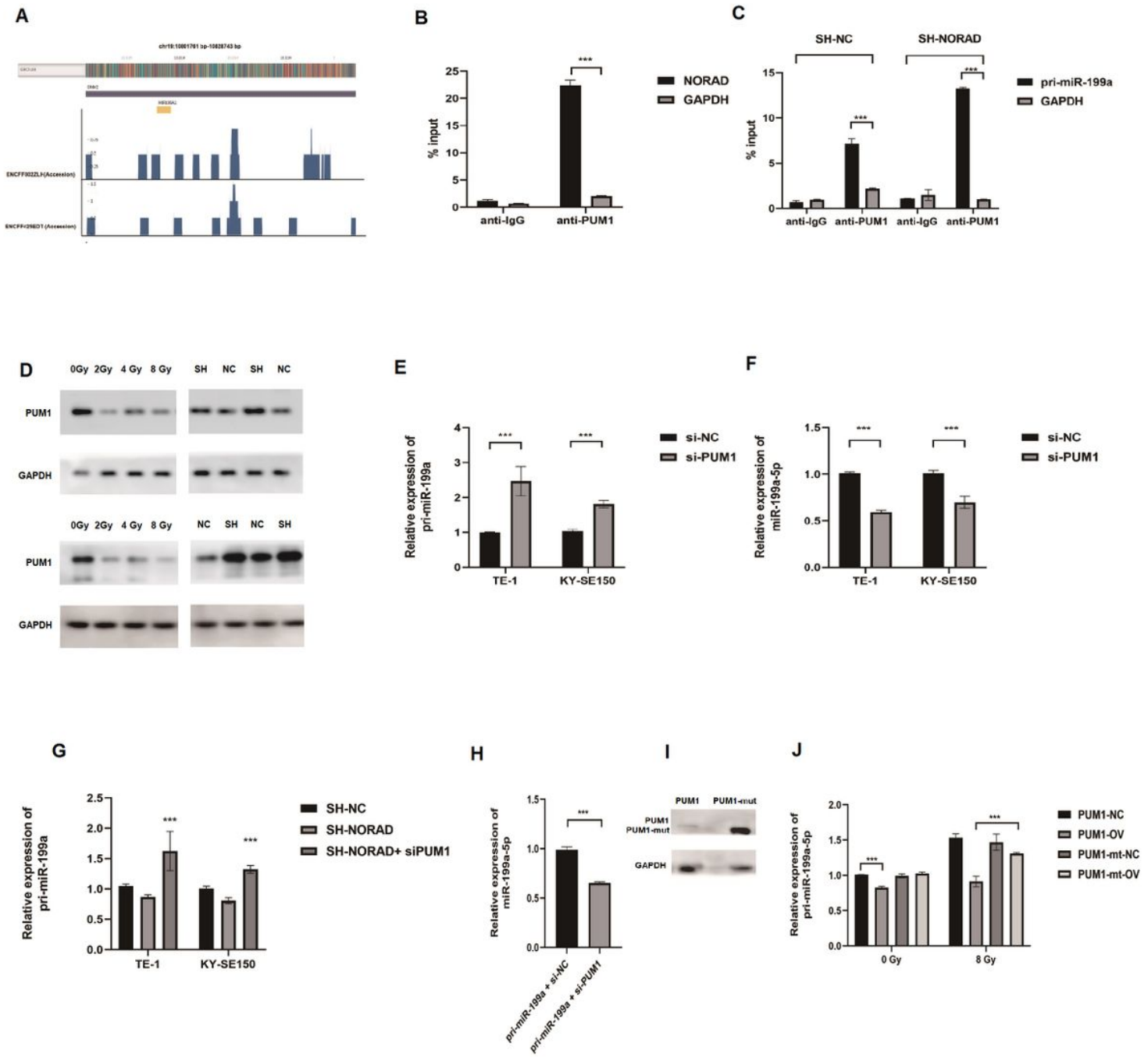


## Figure 7

A. PUM1 CLIP data plotted across pri-miR-199a RNA in K562 cells based on ENCODE datasets. B. qPCR assay on KYSE-150 after RIP performed by using anti-PUM1 or control IgG for detection of NORAD expression. Values were normalized to levels of immunoprecipitated pri-miR-199a-5p by using normal control IgG. C. qPCR assay on KYSE-150 with or without NORAD knockdown after RIP performed by using anti-PUM1 or control IgG for detection of NORAD expression. Values were normalized to levels of immunoprecipitated pri-miR-199a-5p by using normal control IgG. D. PUM1 expression analyzed by western-blot in KY-SE150 and TE-1 with or without 8 Gy MV X-rays treatments and cells with or without

NORAD knockdown. E. qRT-PCR assay to evaluate the expression of pri-miR-199a-5p in PUM1 knockdown or NORAD knockdown cells compared with control cells. F. qRT-PCR assay to evaluate the expression of miR-199a-5p in PUM1 knockdown cells compared with control cells. G. qRT-PCR assay to evaluate the expression of pri-miR-199a-5p in NORAD knockdown cells with or without PUM1 knockdown. H. qRT-PCR to evaluate the expression of miR-199a-5p after PUM1 knock down in HEK293 cells. I. PUM1 expression analyzed by western-blot in KY-SE150 transfected with negative control or PUM1-mutant lacking the RNA-binding domain (PUM1-mut). J. qRT-PCR assay to evaluate the expression of pri-miR-199a-5p in KYSE-150 cells with PUM1 or PUM1-mut overexpression K.The effect of PUM1 or PUM1-mut overexpression on the expression of the pri-miR-199a-5p in cells with 8 Gy MV X-rays treatment. qRT-PCR analysis for the indicated the degradation target mRNAs

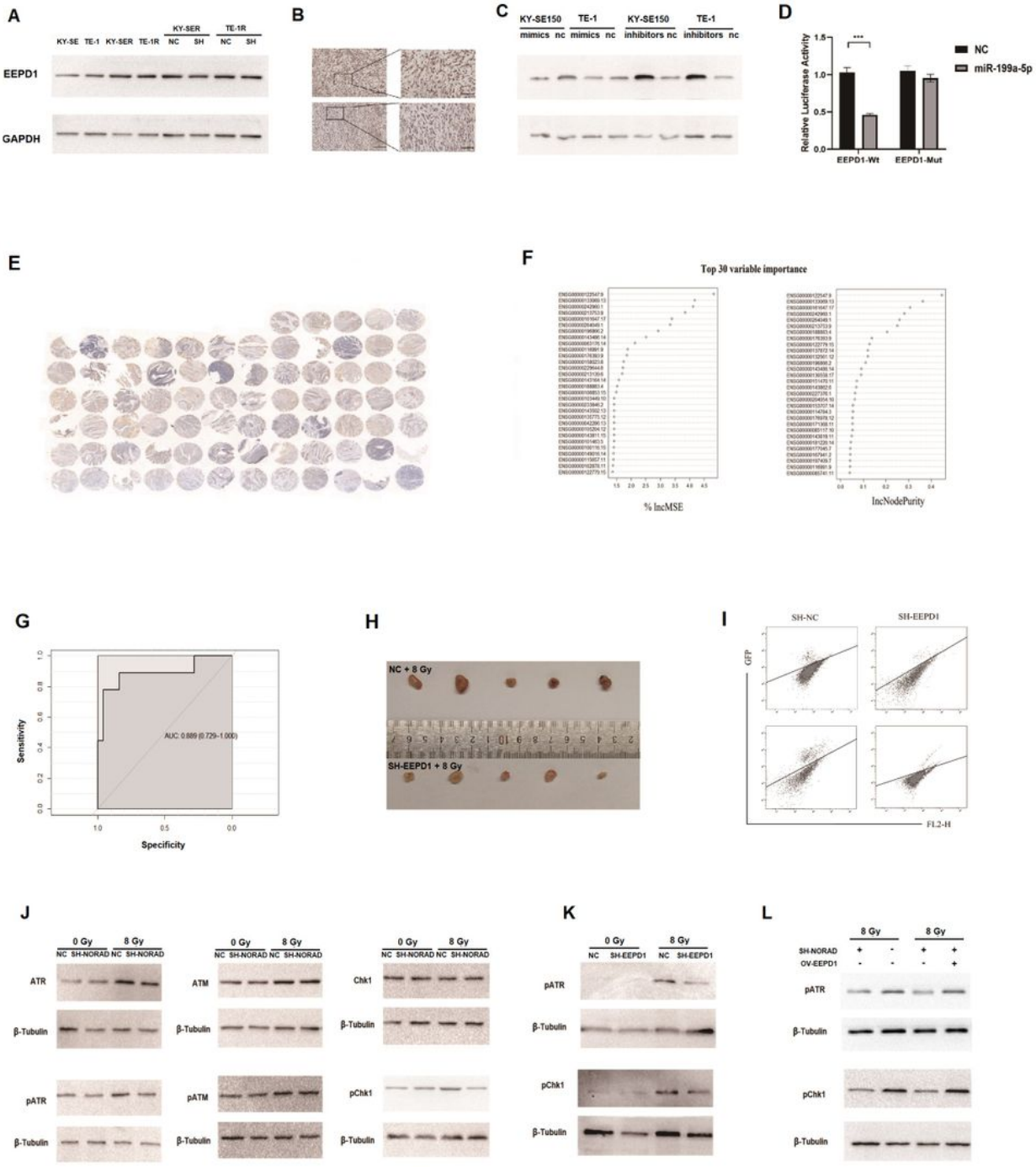


## Figure 8

A. EEPD1 analyzed by western blot in in radio-resistant ESCC cells (KYSE-150R and TE-1R) and their parental cells (KYSE-150 and TE-1); and radio-resistant ESCC cells (KYSE-150R and TE-1R) with or without NORAD knockdown. B. Representative IHC for EEPD1 in NORAD knockdown and control group pf allograft tumors. C. EEPD1 analyzed by western blot in radio-resistant ESCC cells after transducing with miR-199a-5p mimics and miR-199a-5p inhibitors respectively. D. Dual luciferase reporter assay conducted

by co-transfection of wild type or mutant 3'UTR EEPD1 mRNA with miR-199a mimic or negative control into KYSE-150 cells. Luciferase activity are showed as mean ± SEM. E. Immunohistochemistry staining of EEPD1 in 77 ESCC cancer tissues. F. Relative importance of genes for segregating radioresistant ESCC patients from radio-sensitive patients calculated in the random forest. The importance of each gene was ranked by its IncMSC values and IncNodePurity values respectively. G. ROC curve for segregating radioresistant ESCC patients from radio-sensitive patients based on EEPD1 expression. H. The effect of EEPD1 on radiotherapy outcome in ESCC xenografts. Subcutaneous ESCC xenografts were established with SH-EEPD1 cells and SH-NC cells respectively. The tumors were harvested and pictured at 3 weeks after radiotherapy delivery; I. HRR in KYSE-150 and TE-1 cells with or without EEPD1 knockdown, and cells with DSB-induced HRR are represented with the percent GFP positive cells. J. ATM, ATR, Chk1and phosphorylation of ATM, ATR, Chk1 were analyzed by western blot in NORAD knockdown cells and control cells, with or without 8 Gy MV X-rays treatment. K. ATR, Chk1and phosphorylation of ATR, Chk1 were analyzed by western blot in EEPD1 knockdown cells and control cells, with or without 8 Gy MV X-rays treatment. L. ATR, Chk1and phosphorylation of ATR, Chk1 were analyzed by western blot in KYSE-150-SH-NORAD cells with or without EEPD1 overexpression after 8 Gy MV X-rays treatment.

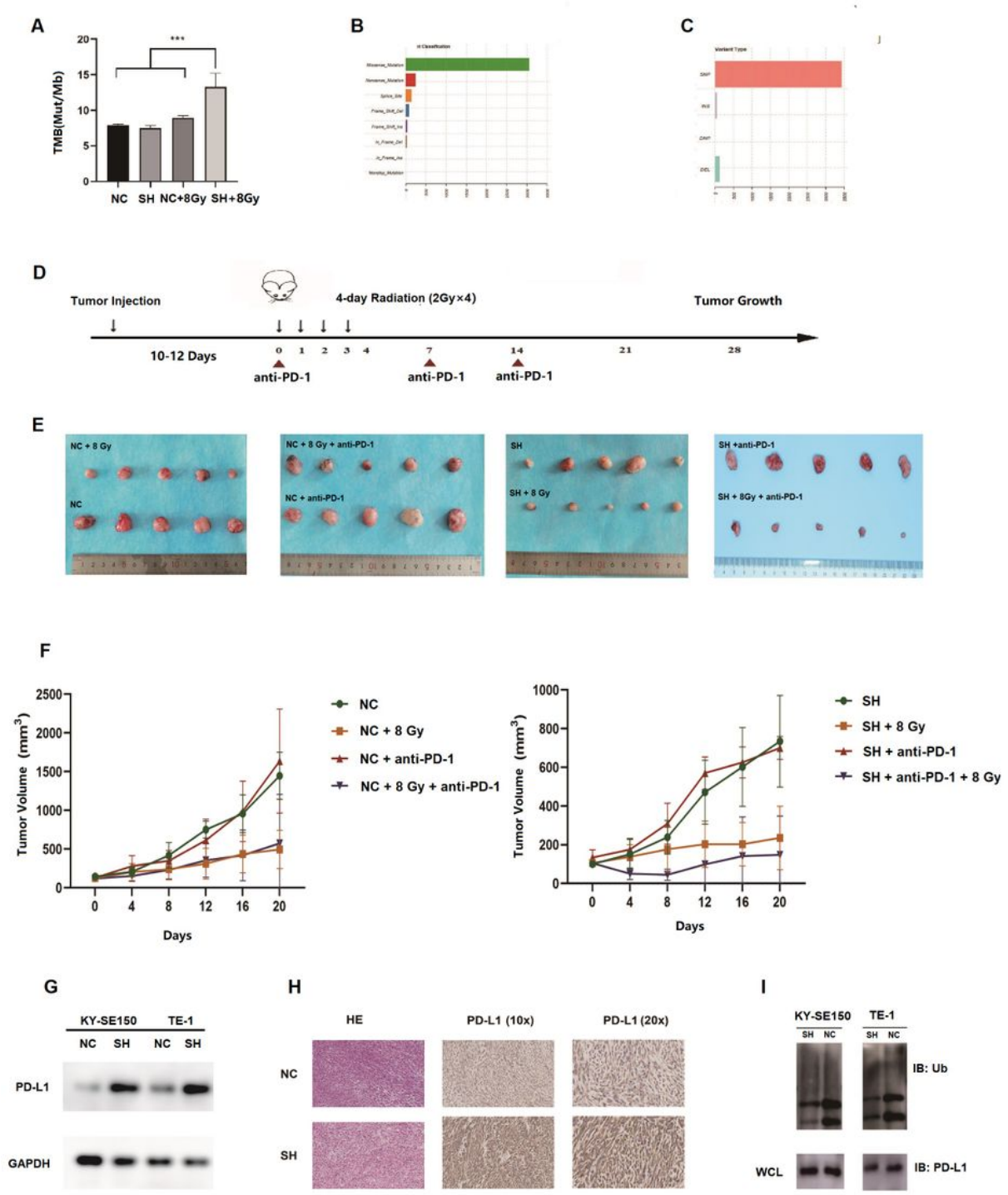


## Figure 9

A. The tumor mutation burden of KYSE-150-sh-nc, KYSE-150-sh-NORAD, KYSE-150-sh-nc+8Gy and KYSE-150-sh-NORAD+8Gy ESCC xenograft tumors. B-C. The mutational classification (B) and variant type (C) for previously ESCC xenograft tumors. D. Scheme for treatments and analyses. 8 Gy radiation was delivered in 4 fractions on consecutive days. Anti-PD-1 antibody was given at the 0, 7,14 days after the first radiation delivery. E. Subcutaneous ESCC xenografts tumors which were established with 1× 107

AKR-SH-NC cells with or without 2 Gy radiation treatment; and subcutaneous ESCC xenografts tumors which were established with 1× 107 AKR-SH-NORAD cells; mice were treated with anti-PD-1 and 4 ×2 Gy radiotherapy or 4 ×2 Gy radiotherapy alone. F. The tumor growth curve in Fig.9E G. PD-L1 expression analyzed by western blot in SH-NC cells and SH-NORAD cells. H. Representative IHC for PD-L1 in NORAD knockdown and control group of allograft tumors. I. Western-blot measurement of PD-L1 pull-down ub derived from the lysates of NORAD knockdown and control radioresistant ESCC cells. Cell were pre-treated with MG132 (20 μM) for 12 hours.

## Supplementary Files

This is a list of supplementary files associated with this preprint. Click to download.

- supplementary1.tif
- supplementary2.tif
- supplementary3.tif